SUPER ROGUE WAVE STATES IN THE CLASSICAL MASSIVE THIRRING MODEL SYSTEM

YANLIN YE[1], LILI BU[1], CHANGCHANG PAN[1], SHIHUA CHEN[1,a], DUMITRU MIHALACHE[2], FABIO BARONIO[3,b]

[1]School of Physics, Southeast University, Nanjing 211189, China
Email:[a] *cshua@seu.edu.cn*
[2]Horia Hulubei National Institute for Physics and Nuclear Engineering,
Department of Theoretical Physics, Bucharest-Magurele, RO-077125, Romania
[3]INO CNR and Dipartimento di Ingegneria dell'Informazione,
Università di Brescia, Via Branze 38, 25123 Brescia, Italy
Email:[b] *fabio.baronio@unibs.it*

Compiled April 6, 2021

Abstract. We obtain the exact explicit super rogue wave solutions of the classical massive Thirring model system, using a nonrecursive Darboux transformation method along with some algebraic manipulations. We reveal that in such a vector system, both rogue wave components, whenever they take the fundamental Peregrine soliton structure or the super rogue wave ones, may possess the same maximum peak-amplitude factor, behaving like those occurring in scalar nonlinear systems. However, due to the coherent coupling, the two super rogue wave components may exhibit drastically different spatiotemporal distributions, despite that they evolve from almost the same background fields. The modulation instability responsible for the rogue wave excitation in such a coupled system is also discussed.

Key words: Super rogue wave, Peregrine soliton, Modulation instability, Massive Thirring model system.

1. INTRODUCTION

The terminology of rogue wave, also known as freak wave, originates from oceanography [1, 2]. It was coined to depict the extreme surface waves occurring in the open ocean, who appear without a presage [3], while carrying a tremendous devastating power that may endanger the cruising ships [1]. Afterwards, scientists and researchers vivified the rogue wave term and referred to it as the one whose amplitude is greater than twice the significant wave height of surrounding waves, but follows an unusual *L*-shaped statistics [4–6]. Nowadays, invoked by the seminal realization of optical equivalents in a microstructured optical fiber [7], this rogue wave concept has unfolded and flourished in many disciplines such as hydrodynamics [8–11], plasma physics [12], nonlinear optics [13–16], acoustics [17], Bose-Einstein condensation [18–20], and even finance [21].

In the context of nonlinear dynamics, rogue waves generally feature a steepsided peak on a nonzero background, accompanied by unusually deep troughs. Such localized structures can be regarded as particular types of solitons or breathers in a broad sense, and mathematically can be described by the rational solutions of the integrable nonlinear partial differential equations [22]. The typical example is the Peregrine soliton, which was first discovered by Peregrine in 1983 as the fundamental rational solution of the focusing nonlinear Schrödinger (NLS) equation [23]. Because of its transient doubly-localized structure, this special type of soliton, sometimes termed *soliton on a finite background* [6], has now been thought of as the prototype of realistic rogue waves [24], and has become a hot topic of intense research in the past decade, on both theoretical [25–28] and experimental sides [8, 12, 29]. Meanwhile, there has also been much research interest in the multiple rogue waves that consist of several Peregrine solitons [30–32] and in the super rogue waves that form as a result of the maximum superposition of three or six Peregrine solitons [33–35].

On the other hand, in a variety of practical scenarios, the physical systems under consideration would involve multiple components of different polarizations and frequencies [36, 37]. When these components interact in a nonlinear manner, complex vector rogue wave dynamics would appear, exhibiting characteristics that are inaccessible to scalar integrable models [22]. As examples, multi-component systems could admit the dark counterpart of optical rogue waves [38], the existence of rogue wave solutions in defocusing nonlinear systems [39], the coexistence of different rogue wave structures on the same background [40], the appearance of anomalous Peregrine solitons in nonlinear media involving the self-steepening effect [41, 42], and the formation of Peregrine rogue waves on a periodic-wave background caused by interference [43], to name a few. This is not surprising as the coupled nonlinear systems can allow the energy transfer among the wave components involved, giving rise to peculiar vector rogue wave dynamics.

The classical massive Thirring model (MTM) system [44] is, in form, one of the simplest integrable vector nonlinear systems. It has some resemblance to the well-known Manakov system [45, 46], but with the group-velocity dispersion and self-phase modulation (SPM) terms being neglected. However, this model involving a simple form does not mean simplicity in physics; it has included the linear coupling term that can induce the effective dispersion, and thus, in principle, supports the formation of solitons, when the induced effective dispersion counterbalances the nonlinear cross-phase modulation (XPM) effect [44, 47]. These properties make the MTM system interesting and appealing, not only in the understanding of Dirac solitons arising in the quantum field theory [48–51], but also in the description of the Doppleron resonance in nonlinear atom optics [52] as well as the soliton propagation in optical Bragg gratings [53–56] or in periodic lattices [57]. As regards this MTM system, the fundamental rogue wave solutions [58, 59] as well as their higher-order versions [60] were reported previously, revealing that such rogue wave states can even be excited in coherent resonant media at extremely low powers [58].

In this paper, we aim to derive the general exact explicit super rogue wave solutions of the MTM equation, which, to the best of our knowledge, were not reported before. Here, for the sake of simplicity, we only consider the super rogue wave states resulting from the nonlinear superposition of three Peregrine solitons, but emphasize that the super rogue waves coming from six or more Peregrine solitons can be derived in a similar fashion. We find that, in such a coupled system, both rogue wave components possess the same maximum peak-amplitude factor, no matter whether they take the fundamental Peregrine soliton or the super rogue wave structures. This is quite different from what one might expect from other vector nonlinear systems, where the fundamental and super rogue waves always feature a variable peak amplitude due to energy exchange [36–42, 46]. Additionally, we will present a study of the modulation instability (MI) for such a vector model and give the condition of existence of these rogue waves. The paper is organized as follows. In Sec. 2, we present the classical MTM system and the corresponding rogue wave solutions. The rogue wave dynamics is investigated in Sec. 3. Our conclusions are given in Sec. 4.

2. THE CLASSICAL MTM SYSTEM AND ROGUE WAVE SOLUTIONS

In an optical context, the MTM system [44,47,53] that governs the propagation of the forward and backward waves in the fiber Bragg gratings can be expressed as

$$\begin{aligned} &i(u_{1t}+vu_{1x})+u_2+u_1|u_2|^2=0,\\ &i(u_{2t}-vu_{2x})+u_1+u_2|u_1|^2=0, \end{aligned} \tag{1}$$

where $u_{1,2}(x,t)$ are the complex envelopes of counter-propagating waves, v is the linear group velocity, and x and t are the laboratory coordinate and time, respectively. Here the subscripts stand for partial derivatives. It is seen that the MTM system contains only two ingredients: the linear coupling and the XPM, denoted by the second and third terms on the left-hand side of Eq. (1), respectively, without taking the group-velocity dispersion and SPM effects into account. This is more obvious when Eq. (1) is equivalently expressed in terms of the light-cone coordinates $\xi = \frac{1}{2}(t+x/v)$ and $\tau = \frac{1}{2}(t-x/v)$:

$$\begin{aligned} &iu_{1\xi}+u_2+u_1|u_2|^2=0,\\ &iu_{2\tau}+u_1+u_2|u_1|^2=0. \end{aligned} \tag{2}$$

Although simple in form, this model still entails the effective dispersion induced by the linear coupling effect and the nonlinearity caused by the XPM term, and therefore admits the complicated soliton or solitary wave solutions. From the point of view of atom optics, such combination of linear coupling and XPM can be realized in resonant nonlinear media involving the electromagnetically induced transparency effect [61] or the Doppleron resonance effect [52], which may lead to the giant enhancement of XPM with the simultaneous suppression of SPM. On the other side, this model is also an example of the nonlinear Dirac equation and was widely used in quantum field theory in the past decades, due to its close relation to the quantum sine-Gordon theory [48–50]. Concerning this model, both the soliton and rogue wave solutions, including their higher order versions, have been obtained [49, 50, 58–60], thanks to its complete integrability [62]. In the following, we are only concerned with the MTM form (2) and proceed to derive its general super rogue wave solutions [33], using the nonrecursive Darboux transformation method [35].

First, one can cast the MTM system (2) into the following 2×2 linear eigenvalue problem:

$$\mathbf{R}_\tau = \mathbf{U}\mathbf{R}, \quad \mathbf{R}_\xi = \mathbf{V}\mathbf{R}, \tag{3}$$

where $\mathbf{R} = [r, s]^T$ (here T means a matrix transpose, and r and s are functions of the variables τ and ξ), and

$$\begin{aligned}
\mathbf{U} &= -\sqrt{\lambda}\begin{pmatrix} 0 & u_1^* \\ u_1 & 0 \end{pmatrix} - \frac{i}{2}\left(\lambda + |u_1|^2\right)\begin{pmatrix} 1 & 0 \\ 0 & -1 \end{pmatrix}, \\
\mathbf{V} &= \frac{1}{\sqrt{\lambda}}\begin{pmatrix} 0 & u_2^* \\ u_2 & 0 \end{pmatrix} - \frac{i}{2}\left(\frac{1}{\lambda} + |u_2|^2\right)\begin{pmatrix} 1 & 0 \\ 0 & -1 \end{pmatrix},
\end{aligned} \tag{4}$$

with λ being the complex spectral parameter and the asterisk indicating the complex conjugate. It is easily shown that the MTM equation (2) can be exactly reproduced from the compatibility condition $\mathbf{U}_\xi - \mathbf{V}_\tau + \mathbf{U}\mathbf{V} - \mathbf{V}\mathbf{U} = 0$.

Then, based on the one-fold Darboux transformation that relates the new solutions with the old ones [59, 60], one can formulate the nth-order rational rogue wave solution of Eq. (2) as

$$\begin{aligned}
u_1^{[n]} &= u_{10}\left(1 - \frac{i}{|u_{10}|}\mathbf{Y}_2\mathbf{M}^{-1}\mathbf{Y}_1^\dagger\right)\left(\frac{\det(\mathbf{M})}{\det(\mathbf{M}^*)}\right), \\
u_2^{[n]} &= u_{20}\left(1 + \frac{i}{|u_{20}|}\mathbf{Y}_2\mathbf{N}^{-1}\mathbf{Y}_1^\dagger\right)\left(\frac{\det(\mathbf{N})}{\det(\mathbf{N}^*)}\right),
\end{aligned} \tag{5}$$

where the dagger † denotes the complex-conjugate transpose, $\det$ means taking the determinant of the matrix, and u_{j0} $(j = 1, 2)$ are the plane-wave seeds defined by

$$u_{10} = a\exp[-i(k\xi + \omega\tau)], \quad u_{20} = b\exp[-i(k\xi + \omega\tau + \pi)], \tag{6}$$

with the amplitudes a and b, the wavenumber k, and the frequency ω obeying the dispersion relations:

$$b = \frac{a}{a^2 + \omega}, \quad k = \frac{\omega}{(a^2 + \omega)^2}. \tag{7}$$

It should be noted that the plane-wave seeds possess the same propagator, except for a phase delay of π at the second component. Here $\mathbf{Y}_{1,2}$ are the $1\times n$ row vectors determined through

$$\left[\begin{array}{c}\mathbf{Y}_1\\ \mathbf{Y}_2\end{array}\right]=[\mathbf{\Phi}^{(0)},\mathbf{\Phi}^{(1)},\mathbf{\Phi}^{(2)},...,\mathbf{\Phi}^{(n-1)}], \tag{8}$$

where $\mathbf{\Phi}^{(m)}$ are the series coefficients of the Taylor expansion of the factorized column vector $\mathbf{\Phi}(\lambda)=\mathbf{G}^{-1}\mathbf{R}(\lambda)$ about the given spectral parameter $\lambda=\lambda_0$ (here $\mathbf{G}=\mathrm{diag}(1,u_{10}/a)$ is a diagonal matrix), and $\mathbf{M}$ and $\mathbf{N}$ are the $n\times n$ matrices whose elements can be obtained via the Taylor expansions of $\mathbf{\Phi}^\dagger\mathbf{X}\mathbf{\Phi}/(\lambda-\lambda^*)$ and $|\lambda|\mathbf{\Phi}^\dagger\mathbf{X}^*\mathbf{\Phi}/(\lambda-\lambda^*)$, respectively, with

$$\mathbf{X}=\left(\begin{array}{cc}\sqrt{\lambda} & 0\\ 0 & -\sqrt{\lambda^*}\end{array}\right). \tag{9}$$

To do this, one can substitute the plane-wave solutions (6) into the Lax pair (3), and find the general form of eigenfunction $\mathbf{R}(\lambda)$, which can be expressed by a linear superposition of two independent vectors $\mathbf{W}_j$ $(j=1,2)$, viz.

$$\mathbf{R}(\lambda)=\mathbf{G}\mathbf{\Phi}(\lambda),\quad \mathbf{\Phi}(\lambda)=\Gamma_+\mathbf{W}_1+\Gamma_-\mathbf{W}_2, \tag{10}$$

where $\Gamma_\pm$ are two arbitrary complex constants, and

$$\mathbf{W}_j=\left[\begin{array}{c}1\\ -\dfrac{i(a^2+\lambda+2\nu_j)}{2a\sqrt{\lambda}}\end{array}\right]e^{i\varphi_j},\quad \varphi_j=\mu_j\xi+\nu_j\tau, \tag{11}$$

with

$$\nu_j=\frac{\omega}{2}+\frac{(-1)^j}{2}\sqrt{a^4-2a^2(\lambda-\omega)+(\omega+\lambda)^2}, \tag{12}$$

$$\mu_j=\frac{(a^2+\omega)(2\nu_j-\omega)+\lambda\omega}{2\lambda(a^2+\omega)^2}. \tag{13}$$

Let now the spectral parameter in Eqs. (10)–(13) be $\lambda=\lambda_0+(\lambda_0-\lambda_0^*)\epsilon^2$ and the complex constants be $\Gamma_\pm=\sum_{j=1}^{n}(\gamma_{2j-1}\pm\frac{\gamma_{2j}}{\epsilon})\epsilon^{2(j-1)}$, where $\lambda_0=\phi^2$, $\phi=a+i\sqrt{\omega}$ $(\omega>0)$, and ϵ and γ_s $(s=1,2,\cdots,2n)$ are arbitrary complex constants. For convenience of discussion, we will term γ_s the structural parameters, as they can affect significantly the spatiotemporal structures of rogue waves under study. In these circumstances, one can expand $\mathbf{\Phi}(\lambda)$ in Eq. (10) into the series in powers of ϵ^2:

$$\mathbf{\Phi}(\lambda)=\mathbf{\Phi}^{(0)}+\mathbf{\Phi}^{(1)}\epsilon^2+\mathbf{\Phi}^{(2)}\epsilon^4+\cdots+\mathcal{O}(\epsilon^{2n}), \tag{14}$$

from which the row vectors $\mathbf{Y}_{1,2}$ can be found by means of Eq. (8). Correspondingly, the element M_{ij} of the matrix $\mathbf{M}$ and the element N_{ij} of the matrix $\mathbf{N}$ can be determined through

$$\frac{\mathbf{\Phi}^{\dagger}\mathbf{X}\mathbf{\Phi}}{\lambda-\lambda^*}=\sum_{ij}^{n}M_{ij}\epsilon^{*2(i-1)}\epsilon^{2(j-1)}+\mathcal{O}(|\epsilon|^{4n}),$$
$$\frac{|\lambda|\mathbf{\Phi}^{\dagger}\mathbf{X}^*\mathbf{\Phi}}{\lambda-\lambda^*}=\sum_{ij}^{n}N_{ij}\epsilon^{*2(i-1)}\epsilon^{2(j-1)}+\mathcal{O}(|\epsilon|^{4n}). \tag{15}$$

As a result, when these matrix expressions are substituted back into Eq. (5), one can obtain the explicit rogue wave solutions for any order n. Usually, the larger the order n, the more complicated form the solutions will take.

One may note that, in contrast to what might be naively expected, the analytical seeking of the rogue wave solutions of the MTM system is not as simple as its form shows. It is seen that the rogue wave solution defined by Eq. (5) takes a more sophisticated form (as two different matrices **M** and **N** are involved therein), compared to those found in other most-studied vector systems [36–43, 46]. This strengthens our belief that the MTM system, although contracted in form, may admit some intriguing rogue wave dynamics unseen in other vector systems.

Below let us write the explicit rogue wave solutions up to the second order ($n=2$), namely,

$$u_1^{[2]}=\left\{1-\frac{i\chi[R_0^*(S_0m_{22}-S_1m_{21})+R_1^*(S_1m_{11}-S_0m_{12})]}{a(m_{11}m_{22}-m_{12}m_{21})}\right\}\times\left(\frac{m_{11}m_{22}-m_{12}m_{21}}{m_{11}^*m_{22}^*-m_{12}^*m_{21}^*}\right)u_{10},$$
$$u_2^{[2]}=\left\{1+\frac{i\chi[R_0^*(S_0n_{22}-S_1n_{21})+R_1^*(S_1n_{11}-S_0n_{12})]}{a(n_{11}n_{22}-n_{12}n_{21})}\right\}\times\left(\frac{n_{11}n_{22}-n_{12}n_{21}}{n_{11}^*n_{22}^*-n_{12}^*n_{21}^*}\right)u_{20}, \tag{16}$$

where $\chi=\lambda_0-\lambda_0^*=i4a\sqrt{\omega}$, and the entry polynomials $m_{ij}=\chi M_{ij}$ and $n_{ij}=$

$\chi N_{ij}/(a^2+\omega)$ are given by

$$\begin{aligned}
m_{11} &= \phi|R_0|^2 - \phi^*|S_0|^2,\\
m_{12} &= \frac{\chi|R_0|^2}{2\phi} + \phi R_0^* R_1 - \phi^* S_0^* S_1 - m_{11},\\
m_{21} &= \frac{\chi|S_0|^2}{2\phi^*} + \phi R_0 R_1^* - \phi^* S_0 S_1^* - m_{11},\\
m_{22} &= \phi|R_1|^2 - \phi^*|S_1|^2 + \frac{\chi}{2}\left(\frac{S_0^* S_1}{\phi^*} + \frac{R_0 R_1^*}{\phi}\right) - (m_{12}+m_{21}),\\
n_{11} &= \phi^*|R_0|^2 - \phi|S_0|^2 \equiv m_{11}^*,\\
n_{12} &= -\frac{\phi^*\chi|R_0|^2}{2\phi^2} + \phi^* R_0^* R_1 - \phi S_0^* S_1 - \frac{\phi^{*2}}{\phi^2} n_{11},\\
n_{21} &= -\frac{\chi|R_0|^2}{2\phi^*} + \phi^* R_0 R_1^* - \phi S_0 S_1^* - \frac{a^2-\omega}{\phi^{*2}} n_{11},\\
n_{22} &= \phi^*|R_1|^2 - \phi|S_1|^2 - \frac{\chi}{2}\left(\frac{\phi^* R_0 R_1^*}{\phi^2} + \frac{\phi S_0^* S_1}{\phi^{*2}}\right)\\
&\quad - \left(\frac{\phi^2}{\phi^{*2}} n_{12} + \frac{\phi^{*2}}{\phi^2} n_{21}\right).
\end{aligned} \tag{17}$$

The other polynomials in Eqs. (16) and (17) are determined by

$$\begin{aligned}
R_0 &= 2(\gamma_1 + \gamma_2\vartheta),\\
S_0 &= -2i\left[\gamma_1 + \gamma_2\left(\vartheta - \frac{2i\sqrt{\omega}}{\phi}\right)\right],\\
R_1 &= \gamma_1\vartheta^2 + \gamma_2\left(\frac{\vartheta^3}{3} + \vartheta - \frac{16ia^2\omega\xi}{(a^2+\omega)\phi^4}\right) + 2\gamma_3 + 2\gamma_4\vartheta,\\
S_1 &= -2i\left[\gamma_1\left(\frac{\vartheta^2}{2} - \frac{2i\vartheta\sqrt{\omega}}{\phi} - \frac{2\omega}{\phi^2}\right) + \gamma_2 q + \gamma_3 + \gamma_4\left(\vartheta - \frac{2i\sqrt{\omega}}{\phi}\right)\right],
\end{aligned} \tag{18}$$

where

$$\begin{aligned}
\vartheta &= 2a\sqrt{\omega}\left[\tau + \frac{\xi}{(a^2+\omega)\phi^2}\right],\\
q &= \frac{\vartheta^3}{6} - \frac{i\vartheta^2\sqrt{\omega}}{\phi} - \frac{2\omega\vartheta}{\phi^2} + \frac{\vartheta}{2} - \frac{8ia^2\omega\xi}{(a^2+\omega)\phi^4} - \frac{i\sqrt{\omega}\phi^{*2}}{\phi^3}.
\end{aligned}$$

In terms of these exact rational solutions given by Eq. (16), general rogue wave dynamics can be demonstrated. As one might check, when $\gamma_2 \neq 0$, these solutions can describe the superposition of three Peregrine solitons, exhibiting the multiple rogue wave patterns or the super rogue wave states, depending on the values of the other three structural structures. However, when $\gamma_2 = 0$ and $\gamma_1 \neq 0$, these solutions become exactly the fundamental Peregrine soliton solutions, always showing three-time peak amplitude relative to their respective background heights, as occurred in a scalar nonlinear system [35].

In the next Section, we will present the simplified fundamental rogue wave solutions and the novel super rogue wave solutions, and then discuss their intriguing rogue wave dynamics.

3. SUPER ROGUE WAVE DYNAMICS AND DISCUSSION OF THE RESULTS

The form of the solutions (16) is compact but less understandable, as it involves many complex parameters and polynomials. As a matter of fact, these solutions can be simplified greatly, by an appropriate translation on the plane (τ, ξ).

For example, when $\gamma_2 = 0$ and $\gamma_1 \neq 0$, one can obtain readily the simplified Peregrine soliton solution by doing the translation operations $\tau \to \tau + \tau_0$ and $\xi \to \xi + \xi_0$ in Eq. (16), where τ_0 and ξ_0 denote the magnitudes of translation along the τ and ξ axes, respectively, given by [35]

$$\begin{aligned} \tau_0 =& \frac{1}{4a\sqrt{\omega}} - \frac{\beta \mathrm{Im}(\gamma_4/\gamma_1)}{4a^2\omega} - \frac{\mathrm{Re}(\gamma_4/\gamma_1)}{2a\sqrt{\omega}}, \\ \xi_0 =& -\frac{\alpha^2}{4a\sqrt{\omega}} + \frac{\alpha^3 \mathrm{Im}(\gamma_4/\gamma_1)}{4a^2\omega}, \end{aligned} \tag{19}$$

with

$$\alpha = a^2 + \omega, \quad \beta = a^2 - \omega. \tag{20}$$

Here, Re and Im denote the real and imaginary parts of a number, respectively. With the above translation operations, the resultant Peregrine soliton solutions can read

$$\begin{aligned} u_1^{\mathrm{Ps}} &= u_{10}\left[1 - \frac{8ia^2\alpha(\theta + 2\omega\alpha\tau) + 4\alpha^3}{4a^2\theta^2 + 16a^4\omega\alpha^2\tau^2 + \alpha^3 - 4i\alpha a^2(\theta - 2a^2\alpha\tau)}\right], \\ u_2^{\mathrm{Ps}} &= u_{20}\left[1 - \frac{8ia^2\alpha(\theta + 2\omega\alpha\tau) + 4\alpha^3}{4a^2\theta^2 + 16a^4\omega\alpha^2\tau^2 + \alpha^3 + 4i\alpha a^2(\theta - 2a^2\alpha\tau)}\right], \end{aligned} \tag{21}$$

where u_{10} and u_{20} are defined by Eq. (6) and

$$\theta = \xi + \alpha\beta\tau. \tag{22}$$

It is obvious that these rational solutions are nonsingular everywhere only when $\omega > 0$, which is therefore deemed as the existence condition of rogue waves.

We emphasize that the resultant solution form given by Eq. (21) does not involve any structural parameters, all of which disappear after these translation operations. Besides, it is shown that both Peregrine soliton components possess the identical three-time peak amplitudes occurring on the origin, as seen in Fig. 1, where we use $a = 1/2$, $b = 2/5$, and $\omega = 1$. This is different from the case in other vector

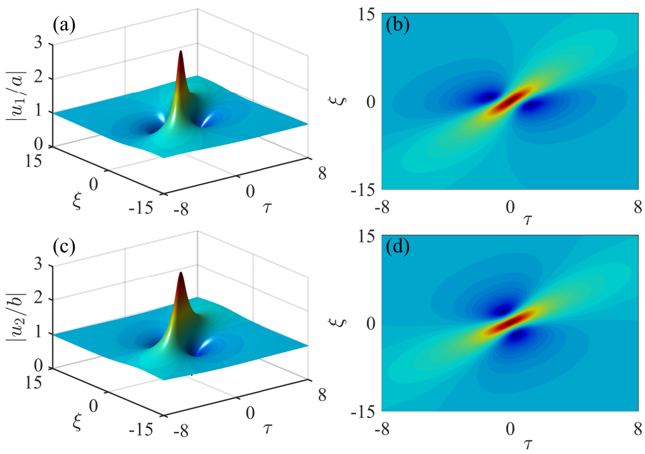

Fig. 1 – Surface (a,c) and contour (b,d) plots of the fundamental Peregrine solitons defined by Eq. (21), obtained with $a = 1/2$, $b = 2/5$, and $\omega = 1$.

systems, in which the rogue wave components may involve variable peak amplitudes [37–43, 46]. We also observe from contour plots that the two Peregrine soliton components have almost the same peak orientation, but drastically different hole orientations, as implied by the fractional polynomials in Eq. (21), which possess the same numerator form but a conjugated pair of denominators.

By comparison, the derivation of the super rogue wave solutions, which occur at $\gamma_2 \neq 0$, from Eq. (16) is quite challenging. We find that, when performing the following translations:

$$\begin{aligned} \tau_0 &= \frac{1}{4a\sqrt{\omega}} - \frac{\beta \mathrm{Im}(\gamma_1/\gamma_2)}{4a^2\omega} - \frac{\mathrm{Re}(\gamma_1/\gamma_2)}{2a\sqrt{\omega}}, \\ \xi_0 &= -\frac{\alpha^2}{4a\sqrt{\omega}} + \frac{\alpha^3 \mathrm{Im}(\gamma_1/\gamma_2)}{4a^2\omega}, \end{aligned} \tag{23}$$

and employing an appropriate value of γ_3, the super rogue wave solutions can be obtained. Usually, to simplify the derivation, one can set $\gamma_2 = 1$ and $\gamma_1 = 0$ in Eq. (23). In this case, the value of γ_3 can be readily found to be

$$\gamma_3 = -\frac{2\omega}{3\alpha^3}(3a^2 - \omega)^2 - \frac{2ia\sqrt{\omega}}{3\alpha^3}(3a^2 - \omega)(a^2 - 3\omega). \tag{24}$$

As a result, the super rogue wave solutions can be expressed as

$$u_1^{\mathrm{srw}} = u_{10}\left(1 - \frac{C + iD}{M - iN}\right), \qquad u_2^{\mathrm{srw}} = u_{20}\left(1 - \frac{G + iH}{M + iN}\right), \tag{25}$$

where C, D, G, H, M, and N are real polynomials, given by

$$C = \frac{192a^4}{\alpha^4}Q\left(Q+\frac{8a^2\zeta\xi}{\alpha^2}\right)+288a^2\left[\iota\tau^2+\frac{2(5a^2-\omega)\tau\xi}{\alpha^2}-\frac{\beta\xi^2}{\alpha^4}\right]-36, \tag{26}$$

$$D = \frac{384a^6\zeta}{\alpha^6}Q^2+\frac{192a^4\beta\zeta^3}{\alpha^6}-72a^2\left(\tau+\frac{9\xi}{\alpha^2}\right)+\frac{768a^4\xi}{\alpha^2}\left(3a^2\tau^2+\frac{3\omega\tau\xi}{\alpha^2}-\frac{\iota\xi^2}{\alpha^4}\right), \tag{27}$$

$$G = \frac{192a^4}{\alpha^4}Q\left(Q+8a^2\tau\zeta\right)+288a^2\left[\frac{\iota\xi^2}{\alpha^4}+\frac{2(5a^2-\omega)\tau\xi}{\alpha^2}-\beta\tau^2\right]-36, \tag{28}$$

$$H = \frac{384a^6\zeta}{\alpha^6}Q^2+\frac{192a^4\beta\zeta^3}{\alpha^6}-72a^2\left(9\tau+\frac{\xi}{\alpha^2}\right)+768a^4\tau\left(\frac{3a^2\xi^2}{\alpha^4}+\frac{3\omega\tau\xi}{\alpha^2}-\iota\tau^2\right), \tag{29}$$

$$\begin{aligned} M = {} & \frac{64a^6}{\alpha^6}Q^3+\frac{48a^4}{\alpha^4}\left(Q-\frac{4a^2\zeta^2}{\alpha^2}\right)\left(Q-16a^2\tau\xi\right) \\ & +\frac{36a^2}{\alpha^2}\left[\frac{(7a^2+3\omega)\zeta^2}{\alpha^2}+4(4a^2-3\omega)\tau\xi\right]+9, \end{aligned} \tag{30}$$

$$N = \frac{12a^2(\xi-\alpha^2\tau)}{\alpha^2}\left[\frac{16a^4}{\alpha^4}Q^2+\frac{8a^2}{\alpha^2}\left(\frac{\iota\zeta^2}{\alpha^2}-4(6a^2+\omega)\tau\xi\right)+9\right], \tag{31}$$

with $\iota = 3a^2+\omega$, $\zeta = \xi+\alpha^2\tau$, and $Q = \zeta^2/\alpha-4\omega\tau\xi$.

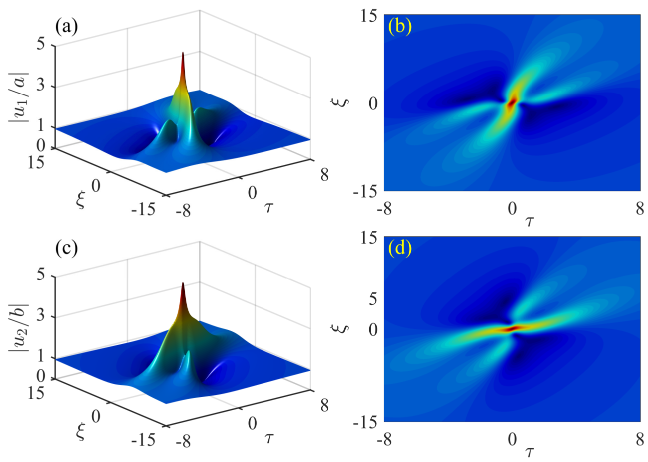

Fig. 2 – Spatiotemporal structures of the super rogue wave solutions given by Eq. (25), obtained with $a = 1/2$, $b = 2/5$, and $\omega = 1$. (a), (c) Surface plots; (b), (d) Contour distributions.

We point out that the super rogue wave solutions obtained above are unique in form, which do not depend on any of structural parameters γ_s. It is seen that these super rogue wave solutions take more complicated solution form, with the numerators in fractional polynomials being also different for two rogue wave components, in comparison with the fundamental Peregrine soliton solutions (21). They always possess the fixed five-time peak amplitude relative to their respective background heights, as occurring in the scalar nonlinear systems [35]. Figure 2 demonstrates such super rogue wave states defined by Eq. (25), using the same background parameters as in Fig. 1. It is shown that apart from the five-time peak amplitude, both rogue wave components feature totally different spatiotemporal distributions, despite the fact that they evolve from almost the same cw backgrounds defined by Eq. (6).

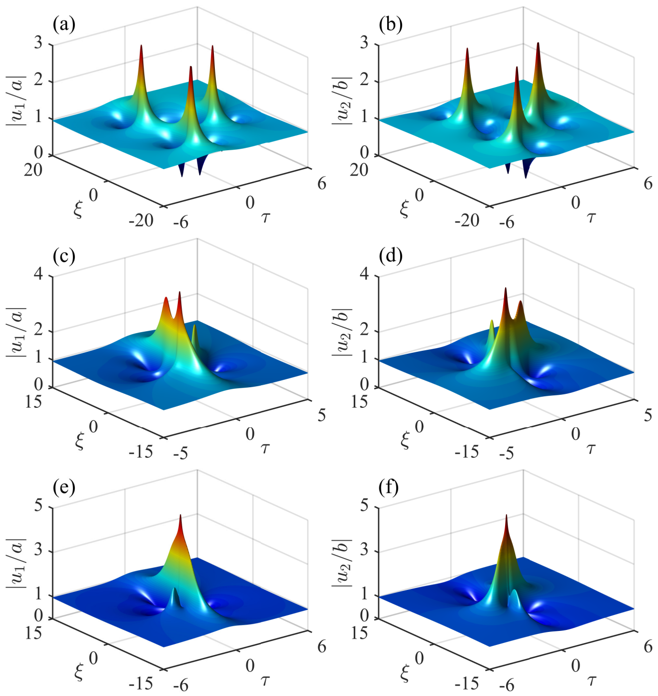

Fig. 3 – Evolution of the superposition of three Peregrine solitons, defined by Eq. (16), from (a), (b) the multiple rogue waves and (c),(d) the composite rogue waves to (e), (f) the super rogue waves, using another set of background parameters $a = 1$, $b = 1/2$, and $\omega = 1$. The structural parameters in each case are specified by (a),(b): $\gamma_2 = 1$, $\gamma_3 = 50$, $\gamma_1 = \gamma_4 = 0$; (c),(d): $\gamma_2 = 1$, $\gamma_3 = 1+2i$, $\gamma_1 = \gamma_4 = 0$; (e), (f): $\gamma_2 = 1$, $\gamma_3 = -1/3+i/3$, $\gamma_1 = \gamma_4 = 0$.

Basically, the formation of second-order super rogue waves is a direct result of the *nonlinear* superposition of three Peregrine solitons. For this reason, the maximum peak amplitude of the superposed rogue waves can never exceed five-fold the background height, as revealed by our analytical solutions (25). Figure 3 shows the

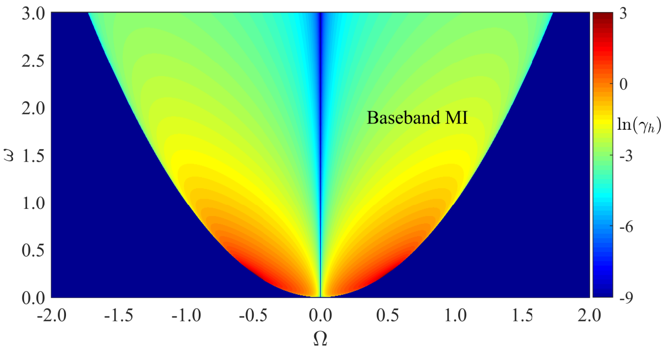

Fig. 4 – Map of the logarithmic MI gain, $\ln(\gamma_h)$, versus Ω and ω for given parameter $a = 1/2$.

evolution of the superposition of three Peregrine solitons, defined by Eq. (6), using the same background parameters $a = 1$ and $\omega = 1$, but different sets of structural parameters. It is exhibited that depending on the choice of structural parameters, the superposed rogue wave states can evolve from the multiple rogue waves [see Figs. 3(a) and 3(b)]) and the composite rogue waves [see Figs. 3(c) and 3(d)]) to the super rogue wave states [see Figs. 3(e) and 3(f)]), with their maximum amplitude factor never exceeding 5.

Lastly, let us find the condition of existence of rogue waves in the MTM system using the baseband MI conjecture, which states that the existence regime of rogue waves coincides with that of the MI of background field as its modulation frequency approaches zero [22, 32, 39]. To do this, one can assume that the background fields are perturbed according to $u_j = u_{j0}\{1+p_j\exp[-i\Omega(\kappa\xi-\tau)]+q_j^*\exp[i\Omega(\kappa^*\xi-\tau)]\}$ $(j = 1,2)$, where p_j and q_j are the complex small perturbation amplitudes, and the parameters Ω and κ denote the real frequency and the complex wave number of the perturbation, respectively. By inserting the perturbed background fields into Eq. (2), one can obtain a system of four linear equations about p_j and q_j, which admits non-trivial solutions only when κ satisfies a quadratic equation:

$$\left[\kappa - \frac{\beta}{\alpha(\Omega^2-\alpha^2)}\right]^2 - \frac{\Omega^2-4a^2\omega}{\alpha^2(\Omega^2-\alpha^2)^2} = 0. \tag{32}$$

As one knows, MI occurs whenever Eq. (32) permits a complex root κ with a nonzero imaginary part. Hence, at a sufficiently low modulation frequency $\Omega \to 0$, this requires $\omega > 0$, which gives the condition for rogue waves to be observable in the MTM system [58]. This result is indeed consistent with the one seen from our analytical solutions (21) and (25), which also requires $\omega > 0$ for arbitrary a. For a clear illustration, we plot in Fig. 4 the map of the logarithmic MI gain, defined by $\ln(\gamma_h) = \ln[|\Omega\mathrm{Im}(\kappa)|]$, versus Ω and ω for $a = 1/2$. It is clear that the gain spectrum displays a baseband MI that could generate rogue waves in the regime of $\omega > 0$, as predicted above.

4. CONCLUSIONS

In conclusion, we presented the second-order super rogue wave solutions of the MTM system, using a nonrecursive Darboux transformation method. It was revealed that in such a vector nonlinear system, both rogue wave components, when taking the fundamental Peregrine soliton structure or the super rogue wave ones, may possess the same peak amplitude factor as compared to their respective background heights, different from many other vector systems in which the rogue wave components may involve variable peak amplitudes due to the energy exchange between them.

In addition, we showed that due to the coherent coupling, the super rogue wave states may feature complicated spatiotemporal distributions for two components, despite that they evolve from almost the same background fields. Finally, we confirmed the existence regime of the rogue waves using the baseband MI theory. We expect that our results obtained for the classical MTM system may help understand the rogue wave dynamics occurring in periodic or Bragg nonlinear optical media [53–56, 58, 61, 63].

Acknowledgements. This work was supported by the National Natural Science Foundation of China (Grants No. 11474051 and No. 11974075) and by the Scientific Research Foundation of Graduate School of Southeast University (Grant no. YBPY1872).

REFERENCES

1. C. Kharif, E. Pelinovsky, and A. Slunyaev, Rogue Waves in the Ocean, Springer, Berlin, 2009.
2. C. Kharif and E. Pelinovsky, Physical mechanisms of the rogue wave phenomenon, Eur. J. Mech. B Fluids **22**(6), 603 (2003).
3. N. Akhmediev, A. Ankiewicz, and M. Taki, Waves that appear from nowhere and disappear without a trace, Phys. Lett. A **373**(6), 675 (2009).
4. M. Onorato, S. Residori, U. Bortolozzo, A. Montina, and F.T. Arecchi, Rogue waves and their generating mechanisms in different physical contexts, Phys. Rep. **528**(2), 47 (2013)
5. J.M. Dudley, G. Genty, A. Mussot, A. Chabchoub, and F. Dias, Rogue waves and analogies in optics and oceanography, Nat. Rev. Phys. **1**(11), 675 (2019).
6. J.M. Dudley, F. Dias, M. Erkintalo, and G. Genty, Instabilities, breathers and rogue waves in optics, Nat. Photon. **8**(10), 755 (2014).
7. D.R. Solli, C. Ropers, P. Koonath, and B. Jalali, Optical rogue waves, Nature (London) **450**(7172), 1054 (2007).
8. A. Chabchoub, N.P. Hoffmann, and N. Akhmediev, Rogue Wave Observation in a Water Wave Tank, Phys. Rev. Lett. **106**(20), 204502 (2011).
9. M. Crabb and N. Akhmediev, Rogue wave multiplets in the complex Korteweg-De Vries equation, Rom. Rep. Phys. **72**(4), 118 (2020).

10. A. Ankiewicz, M. Bokaeeyan, and W. Chang, Understanding general rogue wave solutions of the Gardner equation, Rom. Rep. Phys. **72**(4), 119 (2020).
11. G. Vanderhaegen, C. Naveau, P. Szriftgiser, A. Kudlinski, M. Conforti, A. Mussot, M. Onorato, S. Trillo, A. Chabchoub, and N. Akhmediev, "Extraordinary" modulation instability in optics and hydrodynamics, PNAS **118**(14), e2019348118 (2021).
12. H. Bailung, S.K. Sharma, and Y. Nakamura, Observation of Peregrine Solitons in a Multicomponent Plasma with Negative Ions, Phys. Rev. Lett. **107**(25), 255005 (2011).
13. C. Lecaplain, Ph. Grelu, J.M. Soto-Crespo, and N. Akhmediev, Dissipative Rogue Waves Generated by Chaotic Pulse Bunching in a Mode-Locked Laser, Phys. Rev. Lett. **108**(23), 233901 (2012).
14. N. Akhmediev *et al.*, Roadmap on optical rogue waves and extreme events, J. Opt. **18**(6), 063001 (2016).
15. C. Hou, L. Bu, F. Baronio, D. Mihalache, and S. Chen, Sine-Gordon breathers and formation of extreme waves in self-induced transparency media, Rom. Rep. Phys. **72**(1), 405 (2020).
16. D. Mihalache, Localized structures in optical and matter-wave media: a selection of recent studies, Rom. Rep. Phys. **73**(2), 403 (2021).
17. Y.Y. Tsai, J.Y. Tsai, and L. Iin, Generation of acoustic rogue waves in dusty plasmas through three-dimensional particle focusing by distorted waveforms, Nat. Phys. **12**(6), 573 (2016).
18. Y.V. Bludov, V.V. Konotop, and N. Akhmediev, Matter rogue waves, Phys. Rev. A **80**(3), 033610 (2009).
19. E.G. Charalampidis, J. Cuevas-Maraver, D.J. Frantzeskakis, and P.G. Kevrekidis, Rogue waves in ultracold bosonic seas, Rom. Rep. Phys. **70**(1), 504 (2018).
20. B.A. Malomed and D. Mihalache, Nonlinear waves in optical and matter-wave media: a topical survey of recent theoretical and experimental results, Rom. J. Phys. **64**(5-6), 106 (2019).
21. Z.Y. Yan, Financial Rogue waves, Commun. Theor. Phys. **54**(5), 974 (2010).
22. S. Chen, F. Baronio, J.M. Soto-Crespo, Ph. Grelu, and D. Mihalache, Versatile rogue waves in scalar, vector, and multidimensional nonlinear systems, J. Phys. A: Math. Theor. **50**(46), 463001 (2017).
23. D.H. Peregrine, Water waves, nonlinears Schödinger equations and their solutions, J. Aust. Math. Soc. Ser. B: Appl. Math. **25**(l), 16 (1983).
24. V.I. Shrira and V.V. Geogjaev, What makes the Peregrine soliton so special as a prototype of freak waves?, J. Eng. Math. **67**(1-2), 11 (2010).
25. N. Akhmediev, A. Ankiewicz, and J.M. Soto-Crespo, Rogue waves and rational solutions of the nonlinear Schrödinger equation, Phys. Rev. E **80**(2), 026601 (2009).
26. S. Chen, F. Baronio, J.M. Soto-Crespo, Y. Liu, and Ph. Grelu, Chirped Peregrine solitons in a class of cubic-quintic nonlinear Schrödinger equations, Phys. Rev. E **93**(6), 062202 (2016).
27. F. Baronio, S. Chen, and D. Mihalache, Two-color walking Peregrine solitary waves, Opt. Lett. **42**(18), 3514 (2017).
28. F. Baronio, S. Chen, and S. Trillo, Resonant radiation from Peregrine solitons, Opt. Lett. **45**(2), 427 (2020).
29. B. Kibler, J. Fatome, C. Finot, G. Millot, F. Dias, G. Genty, N. Akhmediev, and J.M. Dudley, The Peregrine soliton in nonlinear fibre optics, Nat. Phys. **6**(10), 790 (2010).
30. A. Chabchoub and N. Akhmediev, Observation of rogue wave triplets in water waves, Phys. Lett. A **377**(38), 2590 (2013).
31. S. Chen, Ph. Grelu, D. Mihalache, and F. Baronio, Families of rational soliton solutions of the Kadomtsev–Petviashvili I equation, Rom. Rep. Phys. **68**(4), 1407 (2016).
32. F. Baronio, B. Frisquet, S. Chen, G. Millot, S. Wabnitz, and B. Kibler, Observation of a group of

dark rogue waves in a telecommunication optical fiber, Phys. Rev. A **97**(1), 013852 (2018).
33. A. Chabchoub, N. Hoffmann, M. Onorato, and N. Akhmediev, Super Rogue Waves: Observation of a Higher-Order Breather in Water Waves, Phys. Rev. X **2**(1), 011015 (2012).
34. A. Chabchoub, N. Hoffmann, M. Onorato, A. Slunyaev, A. Sergeeva, E. Pelinovsky, and N. Akhmediev, Observation of a hierarchy of up to fifth-order rogue waves in a water tank, Phys. Rev. E **86**(5), 056601 (2012).
35. S. Chen, Y. Zhou, L. Bu, F. Baronio, J.M. Soto-Crespo, and D. Mihalache, Super chirped rogue waves in optical fibers, Opt. Express **27**(8), 11370 (2019).
36. F. Baronio, A. Degasperis, M. Conforti, and S. Wabnitz, Solutions of the Vector Nonlinear Schrödinger Equations: Evidence for Deterministic Rogue Waves, Phys. Rev. Lett. **109**(4), 044102 (2012).
37. Y. Ye, Y. Zhou, S. Chen, F. Baronio, and Ph. Grelu, General rogue wave solutions of the coupled Fokas-Lenells equations and non-recursive Darboux transformation, Proc. R. Soc. A **475**(2224), 20180806 (2019).
38. B. Frisquet, B. Kibler, Ph. Morin, F. Baronio, M. Conforti, G. Millot, and S. Wabnitz, Optical Dark Rogue Wave, Sci. Rep. **6**, 20785 (2016).
39. F. Baronio, M. Conforti, A. Degasperis, S. Lombardo, M. Onorato, and S. Wabnitz, Vector Rogue Waves and Baseband Modulation Instability in the Defocusing Regime, Phys. Rev. Lett. **113**(3), 034101 (2014).
40. S. Chen, J.M. Soto-Crespo, and Ph. Grelu, Coexisting rogue waves within the (2+1)-component long-wave-short-wave resonance, Phys. Rev. E **90**(3), 033203 (2014).
41. S. Chen, Y. Ye, J.M. Soto-Crespo, Ph. Grelu, and F. Baronio, Peregrine Solitons Beyond the Threefold Limit and Their Two-Soliton Interactions, Phys. Rev. Lett. **121**(10), 104101 (2018).
42. S. Chen, C. Pan, Ph. Grelu, F. Baronio, and N. Akhmediev, Fundamental Peregrine Solitons of Ultrastrong Amplitude Enhancement through Self-Steepening in Vector Nonlinear Systems, Phys. Rev. Lett. **124**(11), 113901 (2020).
43. Y. Ye, L. Bu, W. Wang, S. Chen, F. Baronio, and D. Mihalache, Peregrine Solitons on a Periodic Background in the Vector Cubic-Quintic Nonlinear Schrödinger Equation, Front. Phys. **8**, 596950 (2020).
44. W.E. Thirring, A Soluble Relativistic Field Theory, Ann. Phys. **3**(1), 91 (1958).
45. S.V. Manakov, On the theory of two-dimensional stationary self-focusing of electromagnetic waves, Zh. Eksp. Teor. Fiz. **65**(2), 505 (1973).
46. S. Chen and D. Mihalache, Vector rogue waves in the Manakov system:diversity and compossibility, J. Phys. A: Math. Theor. **48**(21), 215202 (2015).
47. A.R. Champneys, B.A. Malomed, and M.J. Friedman, Thirring Solitons in the Presence of Dispersion, Phys. Rev. Lett. **80**(19), 4169 (1998).
48. S. Coleman, Quantum sine-Gordon equation as the massive Thirring model, Phys. Rev. D **11**(8), 2088 (1975).
49. S.J. Orfanidis, Soliton solutions of the massive Thirring model and the inverse scattering transform, Phys. Rev. D **14**(2), 472 (1976).
50. L.M. Alonso, Soliton classical dynamics in the sine-Gordon equation in terms of the massive Thirring model, Phys. Rev. D **30**(12), 2595 (1984).
51. A. Contreras, D.E. Pelinovsky, and Y. Shimabukuro, L^2 orbital stability of Dirac solitons in the massive Thirring model, Commun. Part. Diff. Eqs. **41**(2), 227 (2016).
52. G. Lenz, P. Meystre, and E.M. Wright, Nonlinear Atom Optics, Phys. Rev. Lett. **71**(20), 3271 (1993).
53. C.M. de Sterke and J.E. Sipe, Gap solitons, Prog. Opt. **33**, 203 (1994).

54. B.J. Eggleton, R.E. Slusher, C.M. de Sterke, P.A. Krug, and J.E. Sipe, Bragg Grating Solitons, Phys. Rev. Lett. **76**(10), 1627 (1996).
55. B.J. Eggleton, C.M. de Sterke, and R.E. Slusher, Bragg solitons in the nonlinear Schrödinger limit: experiment and theory, J. Opt. Soc. Am. B **16**(4), 587 (1999).
56. A.B. Aceves, C. Deangelis, and S. Wabnitz, Generation of solitons in a nonlinear periodic medium, Opt. Lett. **17** (22), 1566 (1992).
57. T. Xu and D.E. Pelinovsky, Darboux transformation and soliton solutions of the semi-discrete massive Thirring model, Phys. Lett. A **383**(32), 125948 (2019).
58. A. Degasperis, S. Wabnitz, and A.B. Aceves, Bragg grating rogue wave, Phys. Lett. A **379**(14-15), 1067 (2015).
59. A. Degasperis, Darboux polynomial matrices:the classical massive Thirring model as a study case, J. Phys. A: Math. Theor. **48**(23), 235204 (2015).
60. L. Guo, L. Wang, Y. Cheng, and J. He, High-order rogue wave solutions of the classical massive Thirring model equations, Commun. Nonlinear Sci. Numer. Simulat. **52**, 11 (2017).
61. I. Friedler, G. Kurizki, O. Cohen, and M. Segev, Spatial Thirring-type solitons via electromagnetically induced transparency, Opt. Lett. **30**(24), 3374 (2005).
62. E.A. Kuznetsov and A.V. Mikhailov, Complete integrability of 2-dimensional classical Thirring model, Theor. Math. Phys. **30**(3), 193 (1977).
63. V.P. Ruban, Highly nonlinear Bragg quasisolitons in the dynamics of water waves, Phys. Rev. E **77**(5), 055307 (2008).